

Comments of referee #1.

The introduction states that the overall purpose of this study is to improve the surface rain rate retrieval calculated with the BRAIN algorithm from satellite measurements. How this shall be accomplished is not mentioned anywhere in the manuscript.

We propose to rewrite parts of the introduction in order to clarify more context and purpose of this study:

“The French-Indian satellite Megha-Tropiques, launched in 2011, is primarily devoted to improve our knowledge about the life cycle of tropical convective systems over ocean and continents, the environmental conditions for their formation and evolution, their water budget, and the associated water vapor transport. For cloud studies, the most relevant instrument on the Megha-Tropiques satellite is the MADRAS microwave imager with 9 frequencies (18.7 GHz to 157 GHz). Similar satellite missions for tropical cloud studies are TRMM (Tropical Rainfall Measurement Mission, Huffman et al. 2007; Jensen and Del Genio 2003) or SSM/I (Special Sensor Microwave/Imager, Spencer et al. 1989). In order to retrieve the surface rain rate from brightness temperatures measured in the frame of above satellite missions, retrieval algorithms, as for example BRAIN (Viltard et al. 2006), are utilized. These retrieval algorithms have major sources of uncertainty due to the variability of the density of ice crystals in the tropical atmosphere.

With intent to learn more about the variability of crystal density in tropical convective clouds, two aircraft campaigns (presented in more detail in section 2) were associated to the Megha-Tropiques project. The campaigns have been conducted in order to get a better statistical description of the microphysical properties of hydrometeors in Mesoscale Convective Systems (MCS) in tropical regions. “

Since, as this work shows, the retrieved coefficients are highly variable and also differ between the different clouds (here maritime and continental) one cannot readily use the coefficients found in this study for deriving cloud water content (CWC) from other measurements.

This study suggests to determine the variability of the β exponent of the mass-diameter (m - D : $m = \alpha D^\beta$) relationship through the variability of the exponent σ of the surface-diameter (S - D : $S = \gamma D^\sigma$) relationship along the flight track. The S - D relation is a power law which can be directly calculated from the images of optical array probes (here 2DS and PIP) for other relevant data sets. In this study, S - D is calculated with a temporal resolution of 5 seconds by fitting the surface of the hydrometeors as a function of their D_{max} with a power law. Then, either the user has a bulk measurement of IWC to constrain α , or may use the α parameterizations as a function of β , and T , as presented in this study.

ice/water:

For your calculations you assume that all cloud particles are ice. Did you confirm this? Or can you prove that it is a valid assumption, since measurements were clearly taken

at temperatures where clouds could be mixed-phase. Assuming ice when it is water would result in an error in the calculation of the CWC due to the different density.

In order to identify cases where the mixed phase (ice and water) was present, signals of the Rosemount Ice Detector have been analyzed. The RICE probe is in fact a supercooled water detector. We identified only very few and extremely short cases where the RICE probe showed supercooled water, when occasionally crossing young but small updraft cores. These rare data of supercooled water can be easily excluded from $m(D)$ calculations for ice.

Measurement uncertainties:

The instrumentation is described briefly, which is generally ok. However, what is missing is the important description of measurement errors and uncertainties. Every single one of them will propagate into the retrieval of the coefficients of the $m(D)$ power law relationship and thus into the retrieved CWC. Therefore, a detailed discussion about measurement uncertainties and how they affect the retrieval is inevitable.

In detail:

What are the error margins of RASTA? It has huge error bars in Figure 11. What errors occur in the measurements of the cloud particle instruments, e.g. regarding number concentrations and sizes?

RASTA calibration error and measurement error are in general taken together and estimated to 2dBZ. In figure 11, error bars do not represent the uncertainty on the measurements of RASTA, but the standard deviation with respect to the average of all the reflectivities measured in a layer of 5 Kelvin.

The uncertainty in the concentration of hydrometeors is estimated by the probe suppliers to be 20 %. This uncertainty stems mainly from the calculations of the sampling volume (DOF as fct of particle size, TAS), which is a function of particle size. An uncertainty of 20 % on the measured concentration gives approximately an uncertainty on α of about 20 %.

Explanation:

As CWC is “independent” of the particle concentrations (let’s assume an error of 20%):

$$CWC = \int_0^{\infty} N_1(D) \cdot \alpha_1 \cdot D^\beta \cdot dD = \int_0^{\infty} N_2(D) \cdot \alpha_2 \cdot D^\beta \cdot dD$$

then the uncertainty on the concentrations is not a function of diameters. Also the exponent β is not impacting because the uncertainty is available equally for all diameters. Then

$$\text{if } N_1(D) = \left(1 \pm \frac{\Delta N}{N}\right) \cdot N_2(D)$$

$$\text{then } \alpha_1 = \left(1 \mp \frac{\Delta N}{N}\right) \cdot \alpha_2$$

Therefore , an uncertainty of 20 % on the measured concentration gives an estimated uncertainty for α of roughly 20 %.

Under the conditions where the measurements were taken, a high amount of shattering can be expected. A more detailed discussion in this regard would be highly desirable. How much

data had to be removed due to shattering (is there a correction for the loss of data?), and thus, how does that propagate into the CWC retrieval? Can you demonstrate that the methods you use to identify and remove shattering do suffice? And please also give a short description of these methods, do not only cite the corresponding articles (so the reader has to look into those articles to find out what the correction does).

First of all we have to point out that we always try to use most efficient newest probe tips to avoid shattering. This is valid for 2D-S and PIP probes used during the two Megha-Tropiques measurement campaigns. Only after minimizing shattering, we subsequently apply software to cleanse the data from shattered particles, etc. Distinction between natural particles and the particles resulting from the shattering is performed by analyzing the inter-arrival time between two neighboring particles. Occurrences of inter-arrival times are modeled with the help of Poisson distributions. When shattering is present, the probability of the inter-arrival time of shattered particles and the probability of inter-arrival time of the natural particles are modeled by two different Poisson distributions. The analysis is performed continuously with packages of 20000 particles, which allows taking into account the inhomogeneity of clouds along the flight track, especially with significant variations in particle number concentrations. Hence, we can deduce a threshold time which allow to separates the two populations of particles. However, also some of the natural particles can be eliminated, if the two modes are too close to each other. The size distribution is corrected for this. Our method is widely used, and many discussions can be found in further publications. We have decided not to detail the shattering subject here. The details of the algorithm have been presented at the 2012 ICCP conference:

(R. Dupuy, C. Duroure, A. Arthur, and A. Schwarzenboeck. Particle inter-arrival time analysis and shattering removal at high sampling speed and high particle concentration in mesoscale convective system. ICCP International Conference, Leipzig 2012.)

For example figure 1a, illustrates the differences between two PSD (without and with removal of shattered particles $PSD_{diff} = PSD_{with\ shattering} - PSD_{no\ shattering}$).

Figure 1b)-c) et d), shows three individual PSD of 5-second time intervals.

Without applying the anti-shattering algorithm (and compared to the data when the anti-shattering algorithm is applied), surface-diameter relationships are little impacted on average and the exponent β of m-D increases slightly by approximately +4%. The retrieved prefactor α from the measured and simulated reflectivities and PSD is impacted by about +25%, and CWC increases by about +5%.

The error estimation has been performed according to:

$$\frac{100 * \Delta X}{X} = 100 \frac{(X_{withshattering} - X_{withoutshattering})}{X_{withoutshattering}}$$

where X can be α_σ , β_σ and $CWC(\alpha_\sigma, \beta_\sigma)$

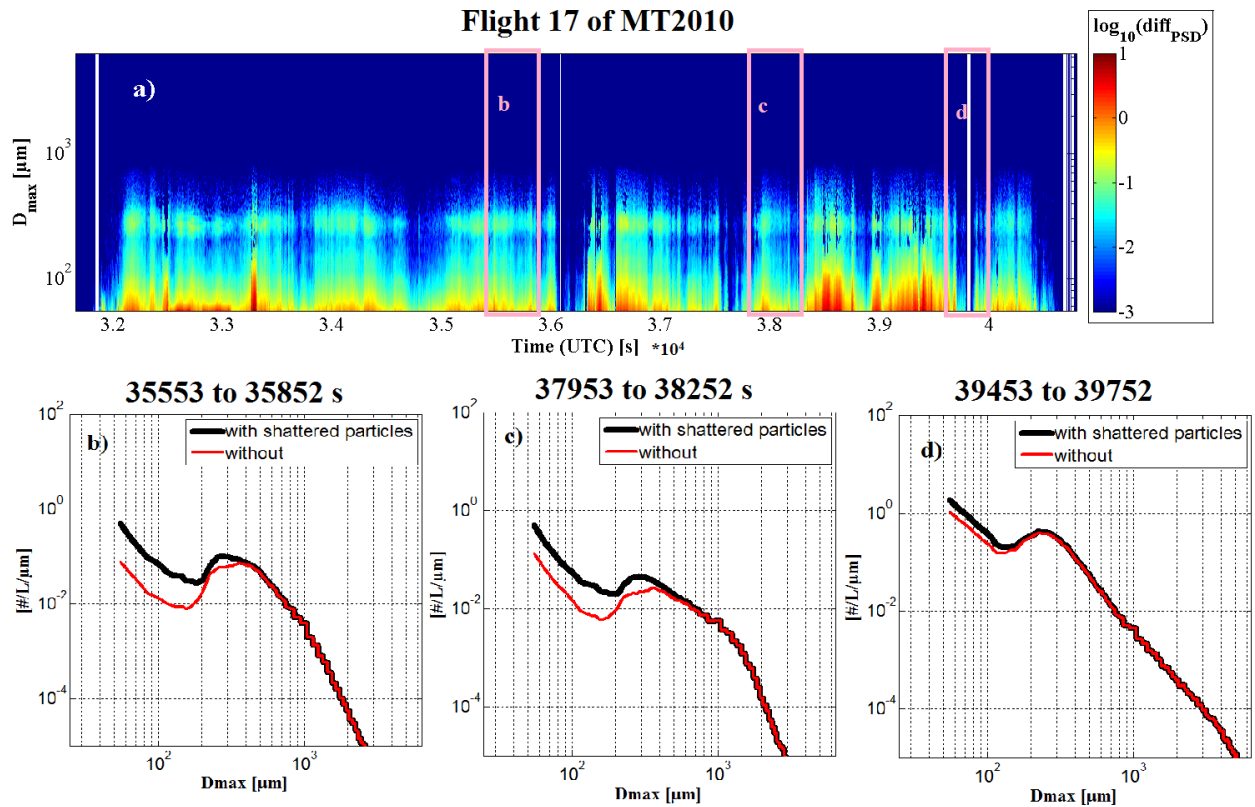


Figure 1 a) Contour plot of the logarithm of PSD containing shattered particles minus the respective PSD where shattered particles have been removed, as a function of the D_{max} on the y-axis and time (seconds after midnight) on the x-axis. 1b-d) in black the PSD containing still the shattered particles, in red PSD after shattering removal.

Full use of dataset:

Furthermore, how do you derive γ (equation10)? Don't you also need γ to derive σ ?

S-D are calculated for 5-seconds steps and are synchronized with PSD and RASTA reflectivity. To calculate S-D, we plot the mean surface of the particles versus their D_{max} (figure2) for the two probes. S-D relation then is fitted by a power law described by two parameters: prefactor γ and exponent σ , for both probes, respectively. On a log-log scale, $\ln(\gamma)$ represents the y-axis intercept and σ the slope of the linear relationship such that $\log(S) = \sigma \cdot \ln(D) + \ln(\gamma)$.

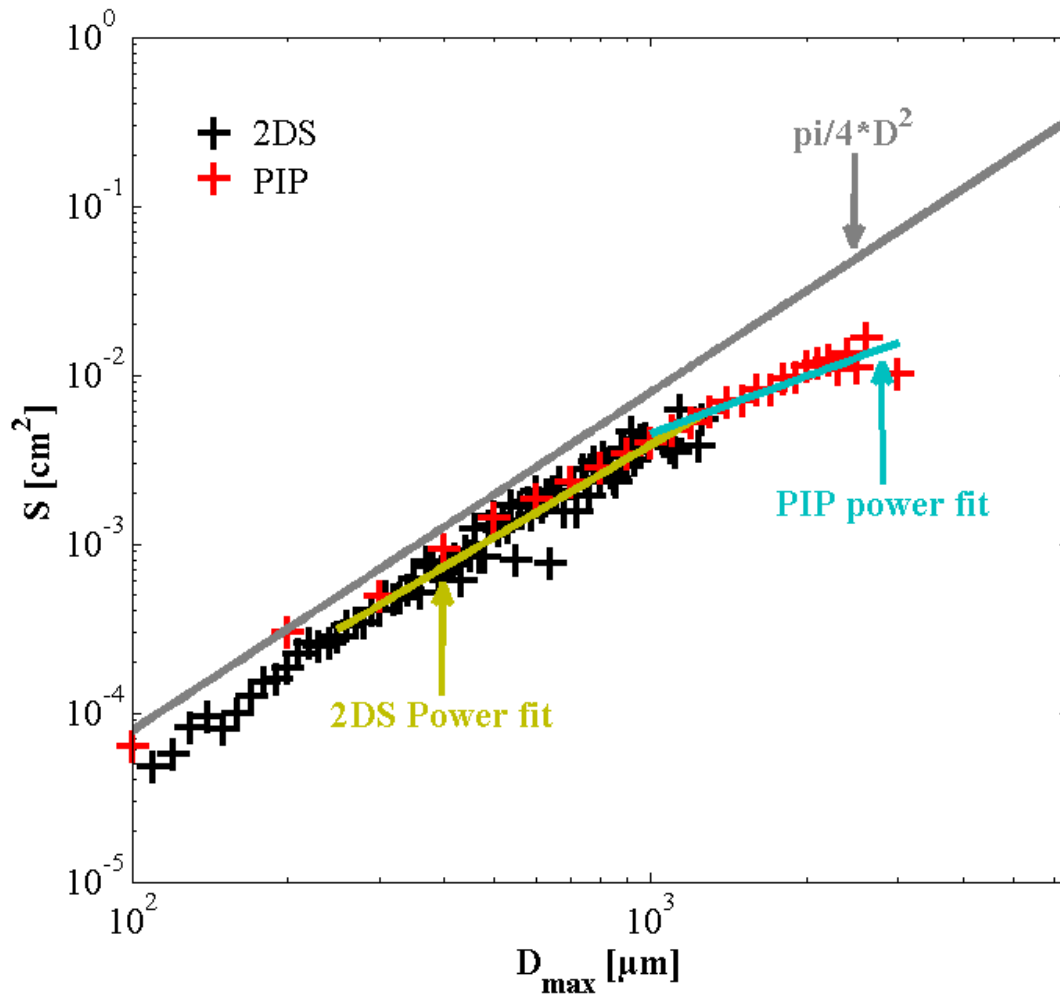


Figure 2 : Mean projected surface in cm^2 on y-axis versus D_{max} in μm on the x-axis. Black symbols represent the 2DS image data and red symbols the PIP data. The grey line would be the power law fit for spherical particles. The golden line is the power law which fits the 2DS data for D_{max} larger than $250\mu\text{m}$ and the blue line fits the PIP data with a power law for D_{max} larger than $950\mu\text{m}$.

In the first instance you use 2DS and PIP measurements to derive α and β . However, from Section 4 on, you only use the 2DS measurements for calculating the surface diameter relationship and use this to derive β . You correctly say that it is better to use 2DS images for sub-millimetric particles, but for the larger crystals you will still gain shape information from the PIP images as well. So, why not using 2DS images for the smaller particles and PIP images for the larger particles?

S-D relationships calculated for sub millimetric (2DS) and millimetric particles (PIP) can deviate. Retrieving m-D relationships for two probe specific (2D-S and PIP) power laws would imply that we need to solve one equation with two unknowns: α_{2DS} and α_{PIP} (eventually three, since we need to know the application range of both m-D relationships in terms of a diameter D_c separating both laws).

$$CWC = \sum_{D_{\text{max}}=55\mu\text{m}}^{D_{\text{max}}=D_c} N(D_{\text{max}}) \cdot \alpha_{2DS} \cdot D_{\text{max}}^{\beta_{2DS}} \cdot \Delta D_{\text{max}} + \sum_{D_{\text{max}}=D_c}^{D_{\text{max}}=6450} N(D_{\text{max}}) \cdot \alpha_{PIP} \cdot D_{\text{max}}^{\beta_{PIP}} \cdot \Delta D_{\text{max}}$$

In the following step for retrieving α , you use again the combined measurements. Wouldn't this be a source of error?

The use of the S-D relationship allows representing the variability of the exponent β of the m-D relationship as a function of the actual 2D images which are recorded. And even if β would be determined from 2D-S images only and thus the exponent β is not carrying most correctly the information of super-millimetric crystals from PIP images, the prefactor α will always somewhat compensate for that. Once the exponent β is estimated from σ as a function of time, the prefactor α is calculated in order that the simulated reflectivity is equal to the measured reflectivity. The prefactor α is constrained such that all the hydrometeors follow the same m-D.

What would the difference be between β_σ when only using 2DS images and β_σ when using images from both instruments?

Calculating a single S-D power law relationship by fitting simultaneously the data points of the 2DS ($250\mu\text{m} < D_{\text{max}} < 1\text{mm}$) and the data points of the PIP ($D_{\text{max}} > 1\text{mm}$) may not produce an ideal and thus realistic S-D power law for the combination of both probes.

Therefore we will introduce for the revised version of the manuscript a σ exponent taking into account simultaneously 2DS and PIP images. This particular σ is calculated by weighting σ of each probe with the ratio of the surface of ice crystals contained in the size range of the individual probe (size range where individual S-D relationship is calculated) over the entire surface within the total size range covered by both probes:

$$\sigma = \frac{\sum_{D_{\text{max}}=250\mu\text{m}}^{950\mu\text{m}} N(D_{\text{max}}) \cdot S(D_{\text{max}})}{\sum_{D_{\text{max}}=250\mu\text{m}}^{6450\mu\text{m}} N(D_{\text{max}}) \cdot S(D_{\text{max}})} \cdot \sigma_{2DS} + \frac{\sum_{D_{\text{max}}=950\mu\text{m}}^{6450\mu\text{m}} N(D_{\text{max}}) \cdot S(D_{\text{max}})}{\sum_{D_{\text{max}}=250\mu\text{m}}^{6450\mu\text{m}} N(D_{\text{max}}) \cdot S(D_{\text{max}})} \cdot \sigma_{PIP}$$

Figures 3 and 4 show the differences of relationships between α_σ and β_σ , when σ is calculated from 2DS and PIP images (figure 3), and when σ is only calculated from images of the 2DS (figure 4).

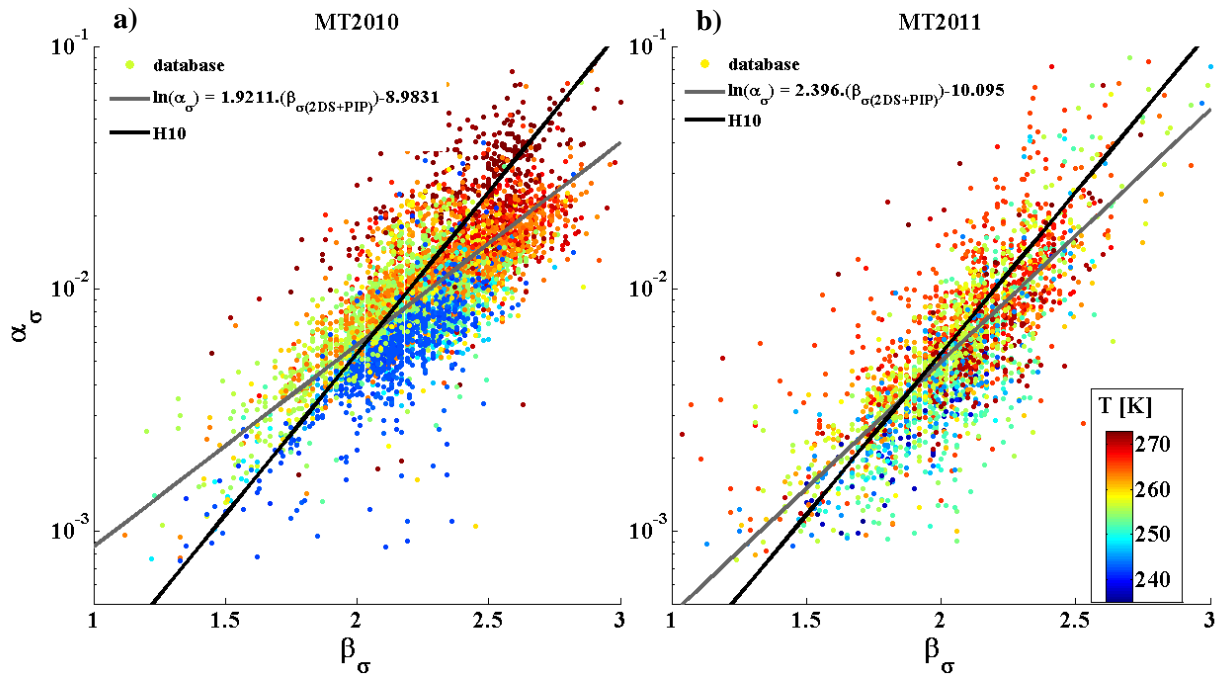


Figure 3 : a) β_σ versus α_σ for MT2010, where β_σ has been derived from σ which is calculated from 2D-S plus PIP images. b) same as a) but for MT2011.

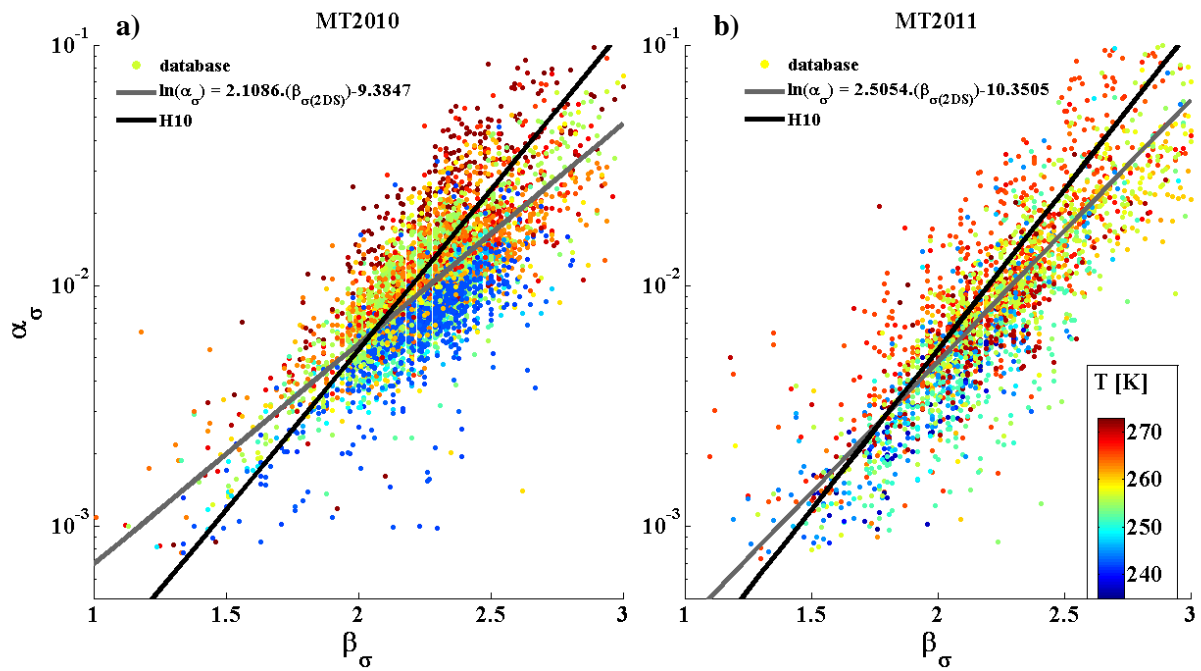


Figure 4 : Same as figure 3, but β_σ derived from σ which is solely calculated from 2DS images.

Specific comments

Page 2984 line 20: “concentrations of the hydrometeors increase with altitude” Please mention to what altitude layer you are referring, other studies have shown the opposite behaviour when looking at higher altitudes. Thus, it is an important additional information.

Also with respect to the comments of the second reviewer we now state in the revised manuscript :

“between the 270K level and the 230K level, the mean profile of the concentration of hydrometeors shows an increase of concentrations with altitude.”

Page 2988 line 15-22: Please indicate the size range covered by the instruments.

“Next to the Doppler Cloud radar RASTA (Protat et al. 2009) in-situ measurements of microphysical properties were performed using a new generation of Optical Array Probes (OAP): the 2-D stereo probe (2DS) from Stratton Park Engineering Company (SPEC) Inc. which allows to monitor 2D images in the size range 10-1280 μm , and the Precipitation Imaging Probe (PIP) from droplet Measurement Technologies (DMT) which measured hydrometeors in the size range from 100-6400 μm .”

Page 2990 line 7: Does it make sense to specify a bin width of 10 microns also in the size range where measurements are purely taken by the PIP? Have you considered an increasing bin width with increasing particle size?

To handle a composite PSD from the two probes, we needed to put them to the same resolution. In order to not lose information given by the 2DS for small sizes of hydrometeors we wanted to keep its resolution (10 μm). Artificially increasing the PIP resolution to 10 μm pixel just keeps all the original information of the 100 μm pixel resolution. No interpolation, just keeping all the information of the original data.

And: No, we did not consider an increasing bin width with increasing particle size.

Page 2992 line 13/14: 2 gm^{-3} of spread in CWC sounds very much. How much is it percentage-wise?

Indeed 2 gm^{-3} of spread in CWC is quite high. But on average the spread is evaluated to be 25% of the retrieved CWC.

Page 2993 line 8-10: What is a typical measurement error for RASTA (besides the mentioned calibration error)?

Calibration error and measurement error are in general taken together and estimated to 2dBZ.

How high are uncertainties in the CWC retrieval if RASTA uncertainties are taken into account?

Related uncertainties are given in table 2. In case that the error due to the calibration is around 2dBZ, this impacts the CWC retrieval by +/- 25%.

Page 2999 line 2/3: While you only use two flights for the analysis for MT2011, I wonder why you don't also use the other two flights stated in Table 1 as a third class – oceanic isolated convective system?

For the isolated oceanic convective systems, relatively few data are available. So for statistical purposes, we consider the dataset of isolated oceanic convective systems not sufficient.

Page 2999 line 14: I am sceptical if you can see a decrease of β_σ with altitude. I would say it is fairly constant, also taking the error bars into account.

“Figure 11b illustrates the trends of β_σ , its mean profile shows a small decrease with altitude for MT2010, but it seems not significant accounting the variability of β_σ at a given altitude.”

Page 2999 line 19: Houze 2004 would be a good reference here.

“MCS systems are composed by a convective part in the front of the systems and a trailing stratiform part (Houze 2004).”

Page 2999 line 24: Are the clouds in SH2010 continental or maritime?

“In addition, our results are compared with two types of vertical profiles given in SH2010. The first profile was obtained from the dataset of the CRYSTAL-FACE project (clouds were formed from land and sea breeze convection in the southern part of Florida; represented by the blue line in figure 11) and the second profile stems from a dataset of ARM (clouds were synoptically generated above the North American continent, Oklahoma ; represented by the dashed blue line in figure 11).

$$m = (0.0102 + 0.00013 \cdot (T - 273.5)) \cdot D^{(2.4+0.0085(T-273.15))} \quad [\text{CRYSTAL - FACE}] \quad (X)$$
$$m = (0.0064 + 0.000095 \cdot (T - 273.15)) \cdot D^{(2.1+0.0036(T-273.15))} \quad [\text{ARM}]$$

“

Page 3000 line 2: You refer to Figure 12d, I assume you mean Figure 11d?

The reviewer is right, however, these parts of the text which describe figure 11 c, d, and f have been deleted, to take into account the comments of the 2nd referee.

Page 3000 line 7-14: I cannot see a general decrease of CWC with altitude for the MT2010 case. I can rather see an increase in the lower levels and than a more or less constant behaviour. A decrease is only visible if you look solely at the uppermost three points.

This part of the text and corresponding figure 12 has been deleted to also take into account the comments of the 2nd referee.

Page 3001 l 5/6: “..., while this decrease is less pronounced for MT2011” - I can hardly see a decrease!

This part of the text and corresponding figure 12 has been deleted to also take into account the comments of the 2nd referee.

Page 3001 line 7/8: “This observational result may be due to low number of samples available in the high altitude during MT2011.” From Figure 11 I still read about 30 samples here (at minimum at 240K). I recommend deleting this sentence.

This part of the text and corresponding figure 12 has been deleted to also take into account the comments of the 2nd referee.

Page 3001 line 22-24: For the decrease in the uppermost part (<245K), are you comparing more than two temperature bins? I would leave this sentence out.

This part of the text and corresponding figure 12 has been deleted to also take into account the comments of the 2nd referee.

Page 3002 line 4-6 (and following part): As you mention, a good correlation between CWC and radar reflectivity is no surprise since you use the reflectivity to derive CWC. So, of what use is this correlation then? Why are you doing it?

Literature provides a lot of Z-CWC relationship at 94GHz (and 35GHZ) where in general CWC has not been constrained by the reflectivity or using only Mie calculations. Hence it is interesting to confront our relationships with other relationships presented in literature for tropical regions.

Page 3004 line 27: As mentioned above, I am not convinced that β decreases in the MT2011 case.

“ It is clearly found that the variability of the $m(D)$ coefficients α_σ and β_σ is large. Mean profiles of this coefficient can be fitted as a function of the temperature (equation X for 2DS+PIP and equation X+1 for only 2DS) and gives smaller values for cold temperatures than for temperatures near the melting layer.

$$\begin{aligned} \text{MT2010:} & \begin{cases} \ln(\alpha) = -0.37459 \cdot T - 14.1809 \\ \beta = 0.008928 \cdot T - 0.041 \end{cases} \\ \text{MT2011:} & \begin{cases} \ln(\alpha) = -0.003306 \cdot T + 0.7431 \\ \beta = 0.0064105 \cdot T + 0.41 \end{cases} \end{aligned} \quad (X)$$

$$\begin{aligned} \text{MT2010:} & \begin{cases} \ln(\alpha) = 0.02999 \cdot T - 12.164 \\ \beta = 0.0025413 \cdot T + 1.61 \end{cases} \\ \text{MT2011:} & \begin{cases} \ln(\alpha) = -0.00018 \cdot T^3 + 0.1341 \cdot T^2 - 33.132 \cdot T + 2715.9 \\ \beta = 5.10^{-5} \cdot T^3 + 0.0037986 \cdot T^2 - 9.4078 \cdot T + 776.66 \end{cases} \end{aligned} \quad (X+1)$$

“

Page 3005: In the discussion about differences between continental and oceanic convective systems, I would appreciate some references to previous studies that show differences in those clouds. E.g. Cetrone and Houze, 2009, Frey et al., 2011.

“Continental MCS in the monsoon seasons are due to the convergence of wet colder air masses from the ocean with dry warmer air masses, while over the Indian Ocean convection is due to the buoyancy of wet air masses leading to weaker convection in our case. Further studies (Cetrone and Houze 2009 ; Frey et al 2011) have discussed differences in the intensity of tropical convection between pure African continental MCS and more maritime MCS with

some continental influence (South Asia to the north of Australia). These studies conclude on deeper convective systems and strongest precipitation for African MCS.”

Page 3006 line 2/3: I think that there are also aggregates visible in the images from MT2011.

“For other levels ice crystal shapes are in general different. Besides aggregates, significant amounts of individual large pristine ice crystals such as dendrites (typically due to water vapor diffusion only) could be observed in MT2011.”

Page 3007/3008: “...and in the fourth L is constant and equal to 16 pixels. L has been chosen out of the size range of [10;100] pixels with 1000 simulations for columns in each of the four cases.” I think one of the “L”s should be a “H”.

“...and in the fourth L is constant and equal to 16 pixels. H has been chosen out of the size range of [10;100] pixels with 1000 simulations for columns in each of the four cases.”

Figure 1:

The line from PIP measurements shows particles smaller 100 μ m, while that is the smallest size detectable for the PIP?!

A pixel is shadowed, when more than 50% of the laser intensity is hidden, then a particle of more than 50 μ m can be represented by one pixel. It is the uncertainty on the size due to the PIP resolution.

In Fig 1b, the PIP distribution starts at about 250 μ m, why is there such a difference in the PIP size range between the distributions in Fig.1a and Fig.1b?

In fact, Fig1b also starts at 50 μ m, but the aspect ratio is equal to 1 between 50 and 150 μ m. The Aspect ratio of particles between 150 μ m and 250 μ m is not valid.

How can the composite distribution differ from the 2DS distribution at sizes around 90 μ m?

This is a mistake of different temporal integration, the time interval taken to plot this quicklook was not exactly the same for various PSDs. The composite PSDs have a time resolution of 5 seconds and the individual raw PSD of 2DS probes and PIP probes have a 1 seconds time resolution. Figures 1a and 1b include only one composite PSD (5seconds) and in addition the mean of 10 individual PSDs of 2DS and PIP probes. This has been corrected in the revised manuscript. New figures are presented below.

While you mention a general good agreement between the two probes, I find the discrepancy in the overlap region at around 100 μ m and at around 1mm not negligible.
Can you comment on these?

The PIP PSD used to produce this figure has been also used to demonstrate the effect of the DOF flag attributed to individual particles (see user’s guide of CIP and PIP instruments from DMT Inc.). The DOF flag allows the user to know if the registered particles was considered

as an out of focus particle or not. Of course we should not have used this one, but the one we use to produce the PSD composite.

In addition, the probability of truncated images of hydrometeors increases with its size. Therefore, for the 2DS as for the PIP, the larger diameter ends of the individual PSDs are noisy. Also the slopes are more important. Even if methods exist (and that we apply to correct for truncated particles), these methods are adapted for spherical particles rather than for complex shapes of ice crystals. The effect of the size reconstruction method (for truncated images) is more visible on the composite of the aspect ratio.

Below are the figure versions of all PSDs over the same 10 seconds of sampling time. In addition, the individual PSD presented for 2D-S and PIP probes are those that are used for the calculation of the composite PSD. We apologize for this mistake, but as this figure was considered just as a schematic quicklook of the method, our attention was not concentrated on that.

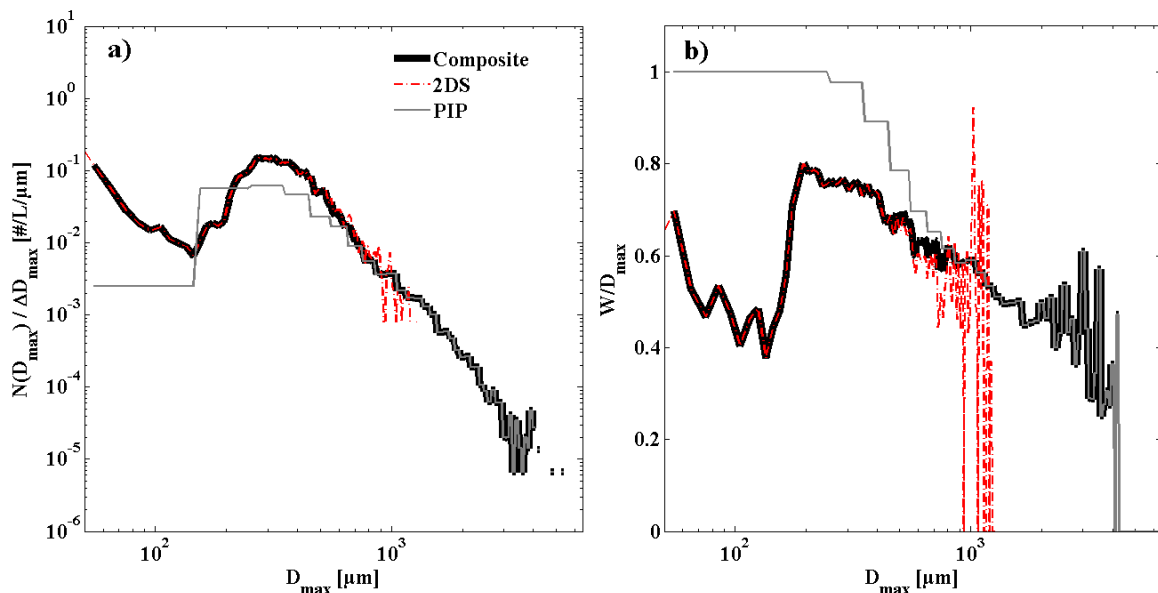


Figure 5 : a) Number size distributions (as a function of D_{max}) of cloud particles. The dashed red line represents the 2D-S data, the grey line the PIP data, and the bold black line represents the composite particle number size distribution (PSD). b) Aspect ratio of 2D particles as a function of D_{max} . Symbols for 2D-S and PIP as above. All curves (number size distributions and aspect ratios) represent an average over 5 seconds of measurements.

Figure 2:

The caption says that you show the effective reflectivity Z_e , while the graph shows Q_{back} . What is correct?

“FIG. 2. Calculated backscattering cross section (in mm^2) as a function of the maximum particle diameter D_{max} (in μm). Pink, blue, green, red and cyan curves are calculated for different Aspect ratios by the T-matrix method, whereas the brown curve is based on the Mie theory calculation for a spherical particle. The black curve represents the Rayleigh approximation. “

Figure 6:

You may want to consider grouping these images according to their habit classes (and specify these on the plot).

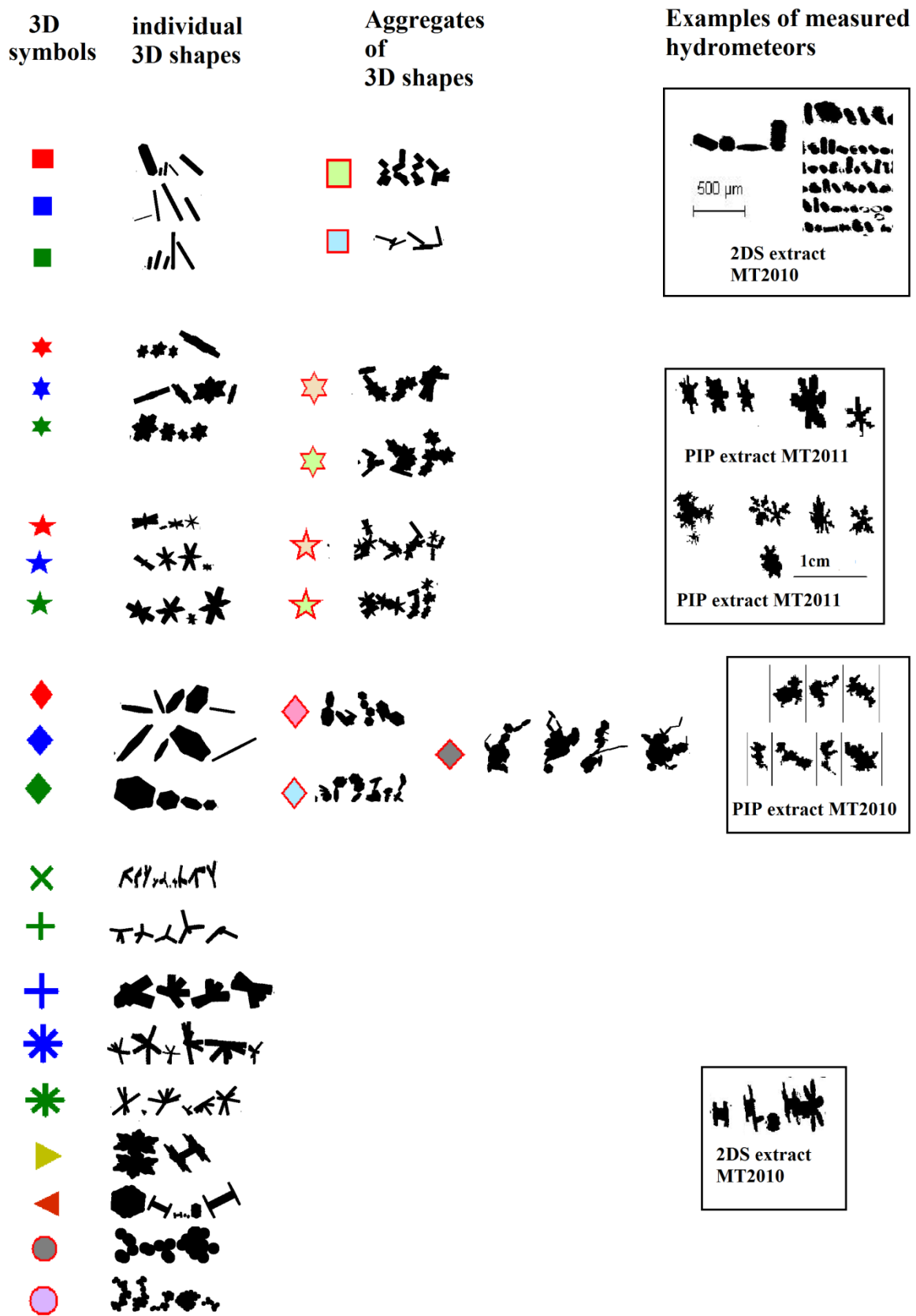


Figure 6 : On the left column are presented examples of 2D projections of randomly oriented 3D shapes of single hydrometeors with their corresponding symbols as they are represented in figure 7 and in table 4. In the middle column, examples of aggregates composed of single individual shapes as shown in the left column. The right column shows examples of crystals resembling what has been recorded in different aircraft measurement campaigns.

Figure 7:

The blue contours around the blue symbols are not recognisable. Changing the colours of the dark blue symbols would be desirable.

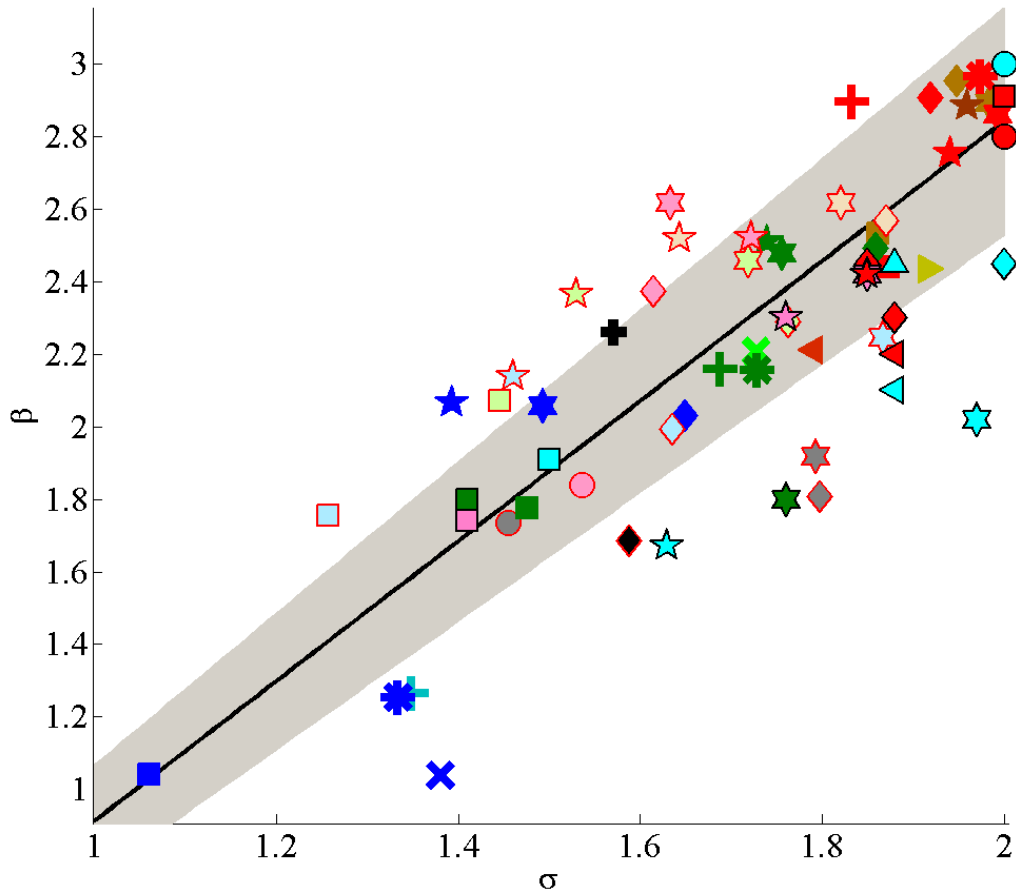


Figure 7 : Exponent β of $m(D)$ relationships as a function of the exponent σ of the corresponding $S(D)$ relationship. Each data point either with red contours or without contours is deduced for a population of 1000 simulated 3D shapes and corresponding projections. Symbols with red contours are deduced for 3D aggregates of crystals of an elementary shape. Symbols with black contours stem from Mitchell (1996). The legend for symbols is given in table 4. A linear fit of all simulated data is shown by the black line. The grey band represents the mean standard deviation (11%)

Figure 8:

Please add the subscript σ on β and α (Fig 8c and d), the caption of Fig 8e says that CWC (black line) is deduced from β_σ and α_σ while the annotation in the Figure suggests it's the average CWC deduced from β_i and α_i . What is correct? Why are there gaps in the black line?

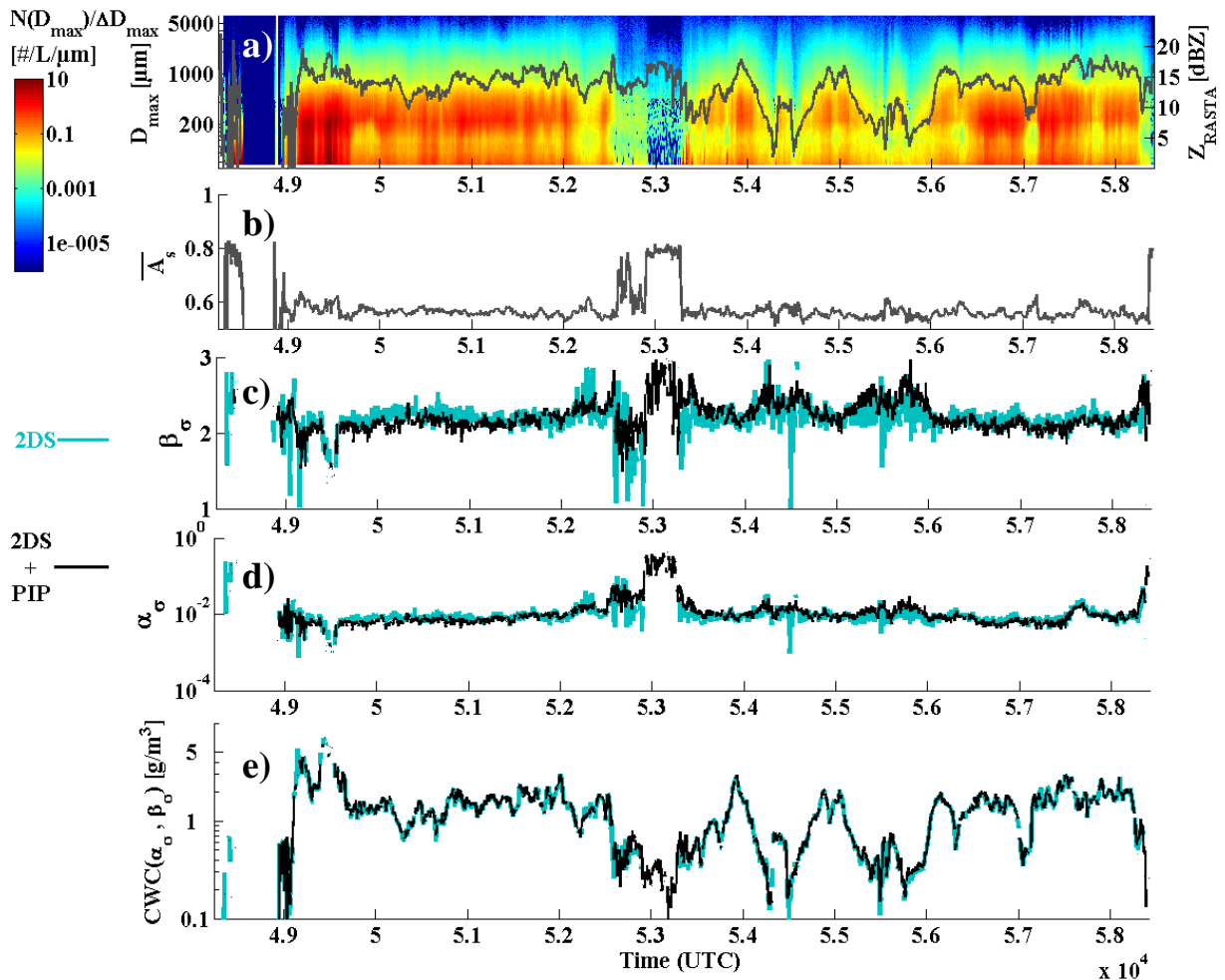


Figure 8 : (a) Contour plot of the time series of the number PSD (as a function of D_{\max}) color coded with the number concentration in $\text{L}^{-1}\mu\text{m}^{-1}$, the grey line shows the simultaneously measured radar reflectivity (secondary y axis). (b) Mean aspect ratio along the flight. (c) β_σ exponent calculated from σ of 2DS in blue and from σ of 2DS plus PIP in black. (d) Pre-factor α_σ , subsequently deduced from the T-Matrix method, for the corresponding β_σ above. (e) CWC calculated with α_σ and β_σ presented above. In blue when $m(D)$ is constrained by the submillimetric images of hydrometeors (2DS) and in black when $m(D)$ is constrained by submillimetric (2DS) plus millimetric (PIP) images of hydrometeors.

Figure 11:

You mention in the text that data points around the melting layer have to be treated with care. Please indicate the melting layer on the plot (e.g. with a shading).

Figures 9 and 10 below are new figures to replace former figure 11. According to the 2nd referee we only keep vertical profiles of the $m(D)$ coefficients. For clarity reasons, we added more details on the standard deviation and the mean profile. Data points are plotted in a kind of background. Figures 9 and 10 are shown, to continue to demonstrate what are the differences when estimating β_σ only from the 2DS probe images (figure 10) and from the images of the two probes (2DS plus PIP).

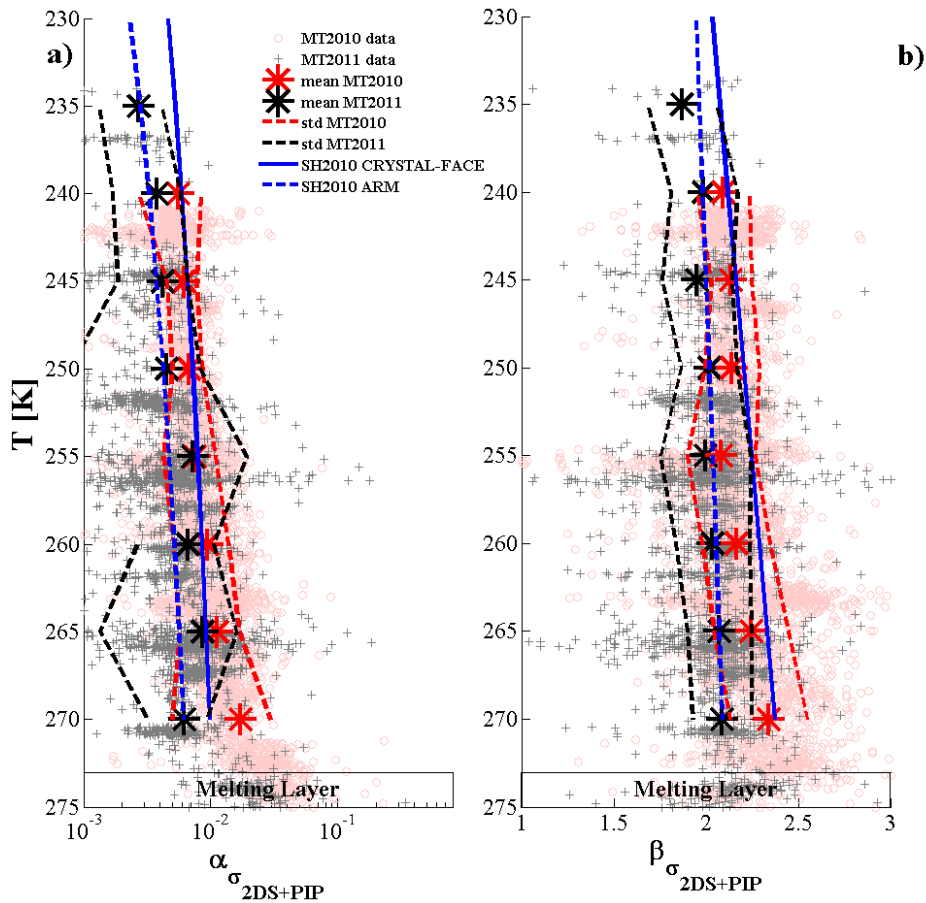


Figure 9 : Vertical profile of $m(D)$ coefficients constrained by T-matrix and the variability of S-D exponent σ calculated from 2D-S plus PIP images. (a) α_{σ} versus the temperature in K. (b) β_{σ} versus the temperature in K. Pink circle show data points (5-seconds time step) of MT2010, grey crosses show MT2011 data. Red and black stars present mean values of $m(D)$ coefficients in 5K temperature intervals for MT2010 and MT2011, respectively. Dashed red and black lines show standard deviations of MT2010 and MT2011, respectively, from the mean value. Blue solid and dashed lines show vertical profiles of SH2010 obtained for CRYSTAL-FACE, and for ARM, respectively.

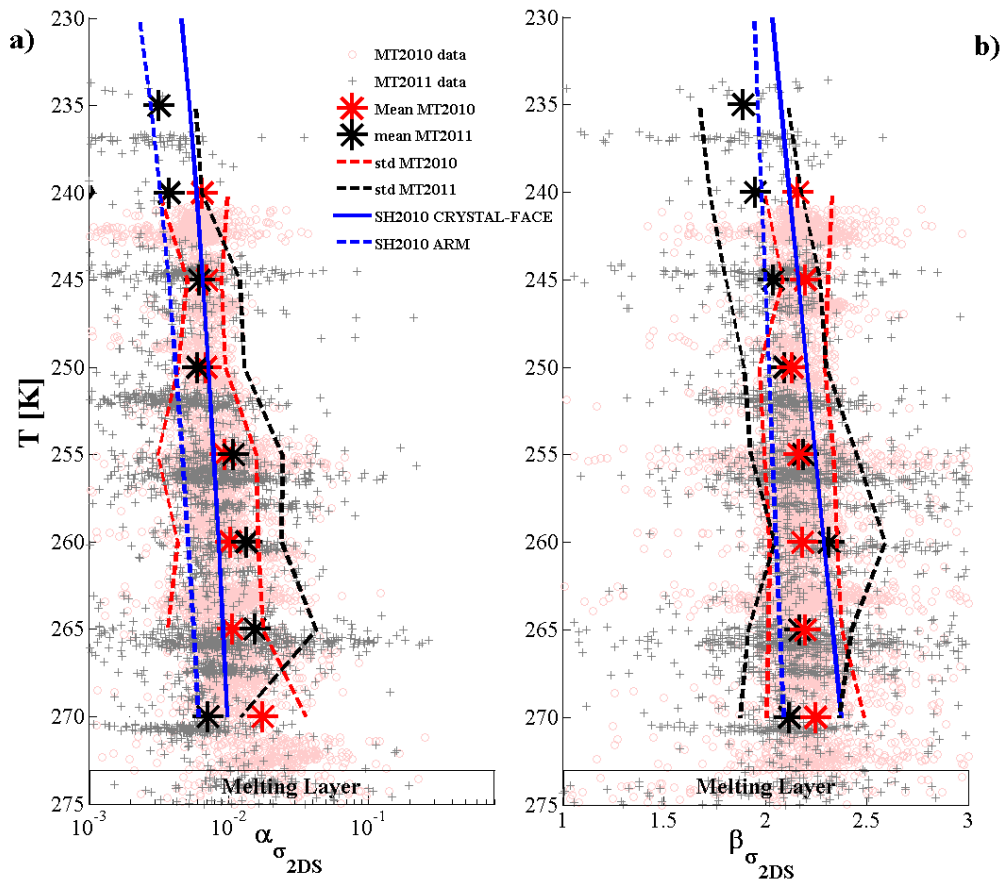


Figure 10 : Same as figure 9, but $m(D)$ coefficients constrained by T-matrix and the variability of S-D exponent σ calculated from 2DS images only.

Why are there no error bars for the total number concentration? Please add.

This part has been deleted according to the 2nd referee comment.

Figure 12g-h:

You write equivalent reflectivity in the caption, in the Figure it says total backscatter coefficient (Q_{back}), what is correct?

This part has been deleted according to the 2nd referee comment.

Figures 11 and 15:

The choice of colours in these figures is unfavourable for colour blind people. You may want to consider another colour pair.

New version is shown above (new figures 9 and 10), and figure 15 has been deleted according to the 2nd referee comment.